

Landslides (2021) 18:2881–2893
 DOI 10.1007/s10346-021-01691-9
 Received: 30 March 2021
 Accepted: 7 May 2021
 Published online: 18 May 2021
 © Springer-Verlag GmbH Germany
 part of Springer Nature 2021

Tapas Ranjan Martha · Priyom Roy · Nirmala Jain · K. Vinod Kumar · P. Sashivardhan Reddy · J. Nalini · S. V. S. P. Sharma · Abhinav Kumar Shukla · K. H. V. Durga Rao · B. Narender · P. V. N. Rao · S. Muralikrishnan

Rock avalanche induced flash flood on 07 February 2021 in Uttarakhand, India—a photogeological reconstruction of the event

Abstract A large debris flow triggered by a rock avalanche in the Raunthi glaciated valley resulted in flash floods in the Rishiganga and Dhauliganga rivers on 07 February 2021 in Uttarakhand, India. Hydel projects, houses, roads and bridges in the path of debris flow were damaged resulting in many deaths. We have used high-resolution satellite data (e.g. Pleiades, WorldView, Kompsat, Cartosat, Resourcesat, Planet) to study the source of flash floods and cause of the slope failure. Our detailed geological assessment, carried out using stereoscopic Pleiades images (50 cm), revealed rock avalanche as the main source of slope failure. The slope failure has exposed a ~197-m-high head scarp near the crown and is controlled by two sets of joints and a foliation that helped in the wedge type failure. The volume of failed mass (rock and ice) estimated by cut and fill method using digital elevation models (DEMs) is ~ 29.3 million m³. The rock and ice descended from a height of ~5474 m and then crashed onto the moraine and ice bridges present in the valley at ~3732 m after travelling ~2.9 km along a steep slope. The heat generated by friction during run out and conversion of potential energy to kinetic energy due to the crashing on valley floor melted snow and ice. The ice melt water along with enhanced snow melting due to high ambient temperature on that day got intermixed with debris and created a slush, which was mobilised as a channelised flash flood. Multi-temporal high-resolution satellite data analysis showed that the debris flow was initiated at ~10:08:45 h (IST), and it travelled with a velocity of ~10.6 m/s. The rock avalanche event lasted for ~50 min, and the crash impact created a severe air blast in the valley. The rock avalanche has also resulted in debris blocking the Raunthi gad valley. Estimated Morphological Obstruction Index (MOI) and Hydro-morphological Dam Stability Index (HDSI) indicate the debris dam to be in an unstable domain.

Keywords Rock avalanche · Landslide dam · Wedge failure · Stereoscopic satellite data

Introduction

A devastating flash flood event occurred along the Rishiganga-Dhauliganga valley on 07 February 2021 in the Chamoli district of Uttarakhand state in India. News report as of 23 February 2021 suggests that around 60 people are dead and 144 people are missing (www.ndtv.com). The flash flood inundated major hydro-electric projects in the Dhauliganga-Rishiganga valley and damaged roads and bridges. The volume of water in the valley during the flash flood was huge, and in the absence of rainfall on that day, it led to an immediate speculation that a glacial lake outburst flood (GLOF) could have been the cause of the debris flow. GLOF is a major hazard in the Himalaya and a potential risk to dams

(Maskey et al. 2020; Shrestha et al. 2010). However, a recent study by Kumar et al. (2021b) did not show any large glacial lake in the Rishiganga catchment having potential to be GLOF. Further, post-disaster satellite images of the catchment area that witnessed the flash flood did not show evidence of GLOF. In contrary, the satellite data analysis found a massive rock avalanche that occurred in the catchment on the western slopes of the Raunthi glacier valley near the Raunthi peak on 07 February 2021, which could have been the potential cause of debris flow and flash flood. In this study, we aim to substantiate this, using high-resolution satellite data acquired before and after the event.

The Uttarakhand state of India is prone to landslides, earthquakes and floods due to its geological and physiographic setup (Martha and Vinod Kumar 2013, Vinod Kumar et al. 2008). Extreme events such as cloud burst in Kedarnath area in 2013 had caused large-scale floods and landslides (Martha et al. 2015). A similar large landslide event had also occurred in Varunawat Parbat at Uttarkashi in the Uttarakhand state, and high-resolution stereoscopic aerial photographs acquired after the event were useful for a detailed geological assessment (Vinod Kumar et al. 2008). In recent times, changing climatic conditions and global warming have led to the melting of glacial ice and snow on mountain ranges, thus triggering a large number of rock avalanches across the world (Dunning et al. 2007; Lagmay et al. 2020). A large and catastrophic rock avalanche occurred at the Xinmo village in the Maoxian county of the Sichuan province of China on 24 June 2017. The avalanche destroyed 64 houses and killed 10 people, and 73 people were reported to be missing (Huang et al. 2019). A giant rock avalanche with a dammed lake was discovered during detailed geological mapping carried out by the Czech Geological Survey in the Western Mongolian Altai (Žáček et al. 2017).

Rock avalanche is a special form of mass movement where a large amount of transported material is dry rock or ice that is fragmented before or during the slope failure. This definition excludes debris as source material but includes any kind of rock, sedimentary, metamorphic, igneous and also pyroclastic deposits (Collins 2014; Hungr and Evans 2004). Such massive mass wasting (in order of million cubic meter) phenomenon has been observed and studied in detail in various parts of Alpine and Himalayan mountains. Rock avalanches first became recognised in Switzerland in the 19th century, when the Elm and Goldau events killed many people, surprisingly long away from the origin of the landslide (Buss and Heim 1881). Large rock avalanches are usually associated with massive air blasts that magnify the damage caused by the landslide itself. The energy involved in the downslope transportation of the rock mass is transformed into kinetic energy,

friction, soil deformation and rock fragmentation; this energy dissipates until the rock mass comes to a stop (Penna et al. 2020). The Langtang debris avalanche in Nepal in April 2015 induced by the M_w 7.8 Gorkha earthquake completely obliterated the village of Langtang and caused an air blast which destroyed stone and wooden houses as well as induced human casualties (Kargel et al. 2016). Uprooted and snapped off trees lay upstream and downstream of the impact area in Langtang. Another potential effect of rock avalanche is damming of the valley due to debris (Dong et al. 2011). Landslide damming is a natural process occurring in narrow valleys and forms when the landslide debris reaches to valley floor blocking the river path (Dai et al. 2005; Gupta and Sah 2008; Delaney and Evans 2015; Li et al. 1986; Costa and Schuster 1988; Takahashi and Nakagawa 1993; Stefanelli et al. 2016; Kumar et al. 2019). Prediction of potential landslide dams and their stability in narrow valleys can be carried out using landslide damming index. Dam slopes, volume and morphology of the valley area are important parameters required to study the landslide dam stability (Stefanelli et al. 2016).

In this paper, we present a photogeological assessment of the rock avalanche that caused the devastating flash flood in

Uttarakhand. Such an event of this scale and magnitude is hitherto less recorded in Indian Himalayas. We have analysed stereoscopic Pleiades imagery acquired after the disaster to delineate the geological controls that lead to the failure of the massive rock wedge. We reconstructed the chain of events and time stamped the event sequence based on photogeological study using geomorphic evidences identified from multi-temporal satellite data. We have identified potential unstable zones, i.e. landslide dams which have resulted from the impact of the rock avalanche and subsequent debris flow.

Study area

The source of the flash flood is located in the Raunthi glacier valley (Raunthi gad) in the Chamoli district of Uttarakhand state in India. Rishiganga further meets Dhauliganga near Raini village (GSI 2021). A synoptic view of the region with origin of the debris flow from the crash zone is shown in Fig. 1. The rock avalanche zone comprises metamorphic rocks such as migmatite gneiss with marble bands surrounded by gneiss, kyanite schist, quartzite, calc silicate of Proterozoic age (Fig. 2). The Rishiganga river carried big chunks of boulder, mud from the Raunthi gad to the Dhauliganga,

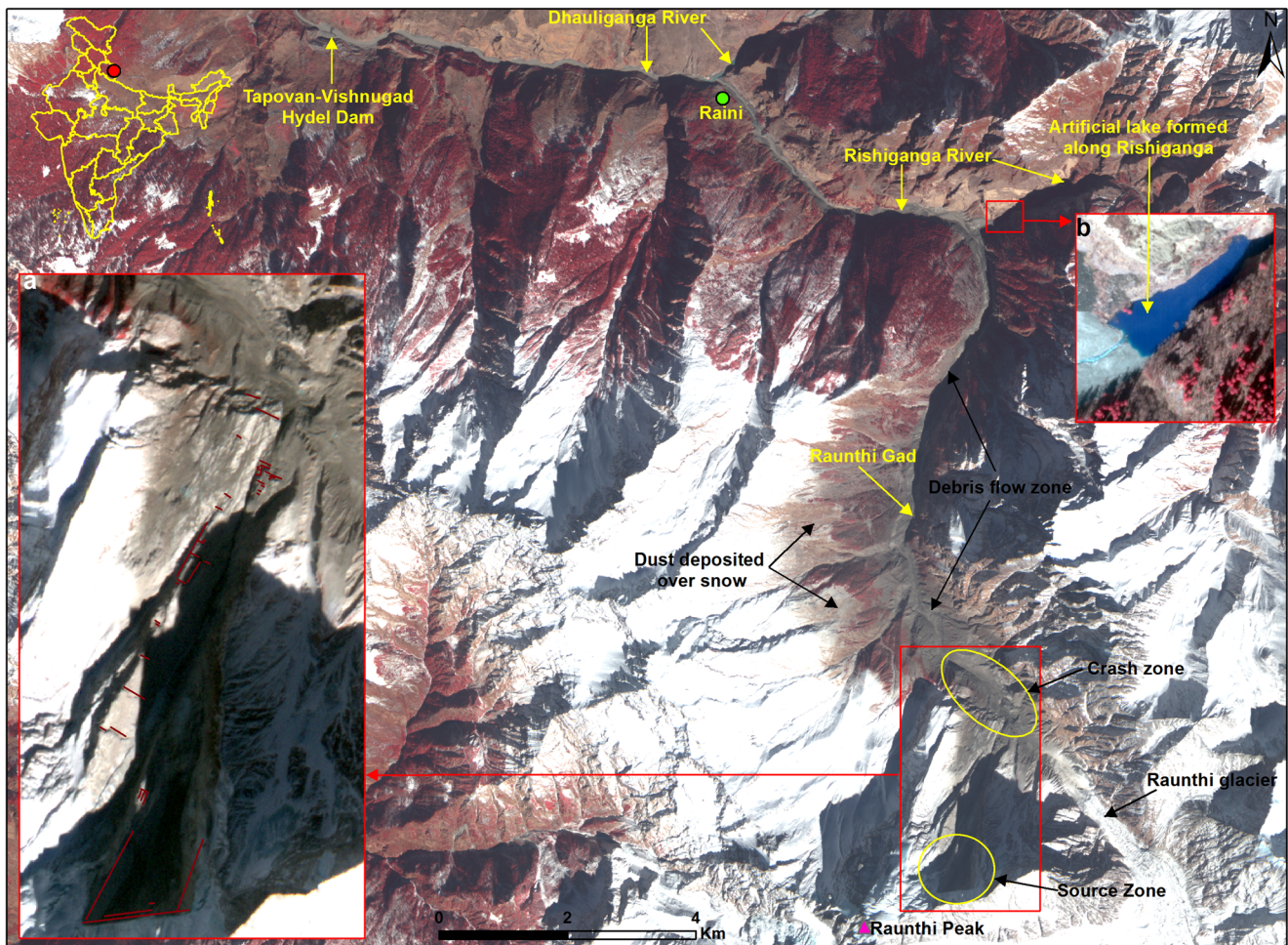


Fig. 1 Synoptic view of the affected region as seen from Resourcesat-2A LISS IV image (08 February 2021) shown in FCC. Inset (a) shows enlarged view of the rock avalanche zone with joints and foliation (red lines), and SkySat-7 image (26 February 2021) in inset (b) shows lake formed due to a landslide dam at the confluence of Rishiganga river and Raunthi gad

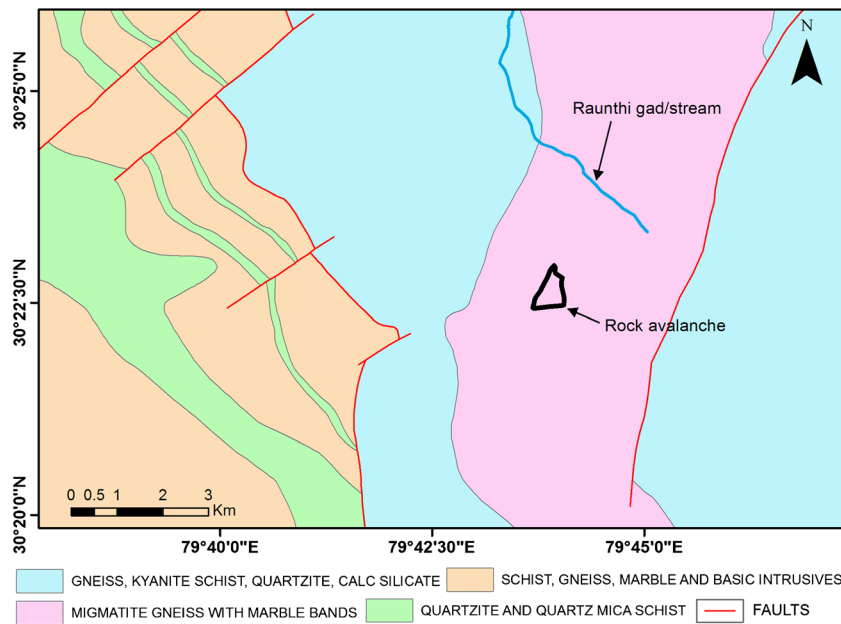


Fig. 2 Geological map of the area around the rock avalanche zone (Bhukosh 2021)

which has damaged Rishiganga and Tapovan-Vishnugad hydroelectric projects, settlements, roads and bridges in and around Tapovan, Raini and Joshimath (Fig. 1). It has also formed an artificial lake at the confluence of Raunthi gad and Rishiganga due to blockage by debris. This lake water is now flowing over the landslide dam (Fig. 1).

Data and method

Satellite data and DEM

Multi-temporal high-resolution satellite data over the affected region captured before and after the event were used in this study (Table 1).

Method

Satellite data interpretation

The area affected by the rock avalanche and the debris deposition was studied mainly using stereoscopic Pleiades data acquired on 10 February 2021. Photogeological interpretation of the affected area was carried out to map the joint and foliation planes, crown of the rock avalanche and its flow path, debris deposition, air blast zone etc. Area affected by the air blast caused due to rock avalanche was identified by mapping the snapped and uprooted trees. Very high-resolution Kompsat-3A and WorldView-2 data acquired before the event were referred, to map these changes.

Reconstruction of event sequence

The rock avalanche has occurred in a remote place and only got noticed by villagers far away from the source region, when the consequent debris flow travelled downstream. There was no direct information immediately available on the cause and source region of the debris flow. Multi-temporal high-

resolution Planet-1 satellite data acquired after the event were mainly used to reconstruct the chain of events. The debris flow front lobe was captured twice (T1-10:31:51 hrs and T2-10:58:35 h) by Planet-1 satellite in the valley. The distance travelled by the debris flow between T1 and T2 along the valley was used to estimate the flow velocity. Subsequently, the distance from the location of debris flow at T1 to the rock avalanche crash zone was measured, and assuming a uniform debris flow velocity, the origin time of debris flow at the crash zone was approximately estimated. Further, geomorphic and image signatures were used for time stamping of the event sequence.

DEM generation and volumetric analysis

Stereoscopic Cartosat-1 and Pleiades-1B data were used to generate DEM of the pre- and post-rock avalanche zones, respectively. The Rational Function Model (RFM) using the Rational Polynomial Co-efficients (RPCs) was used for block triangulation by photogrammetric method (Grodecki and Dial 2003). A single block for both the stereoscopic satellite data with a common reference frame was created using ERDAS © photogrammetric software. The match points generated for both the datasets were converted to a 10-m (Cartosat-1) and 2-m (Pleiades-1B) gridded DEM. Cut and fill method was used to estimate the volume of the rock and ice detached from the source region (Martha et al. 2010). DEM differencing was used to find the height of the failed mass within the release area.

Landslide dam stability evaluation

Landslide damming index was used to determine potential instability of landslide debris dam near the crash zone (Kumar et al. 2021a). To study the potential landslide dam formation in the case of slope failure and its stability

Table 1 List of satellite data used in this study

Sl. no.	Satellite (resolution)	Date	Sources
<i>Pre-disaster</i>			
1	WorldView-2 (46 cm)	28 September 2015	USGS
2	Resourcesat-2A LISS IV Mx (5.8 m)	10 October 2017	ISRO
3	Resourcesat-2 LISS IV Mx (5.8 m)	27 November 2017	ISRO
4	Cartosat-1 Stereoscopic (2.5 m)	01 November 2018	ISRO
5	Kompsat-3A (55 cm)	16 September 2020	KARI
6	Sentinel-2A (10 m)	05 February 2021	ESA
<i>Post-disaster</i>			
7	Planet-1 (3 m)	07 February 2021	Planet Labs
8	Resourcesat-2 LISS IV (5.8 m)	08 February 2021	ISRO
9	Resourcesat-2 LISS III (23.5 m)	08 February 2021	ISRO
10	Pleiades-1A Monoscopic (50 cm)	09 February 2021	CNES
11	Pleiades-1B Stereoscopic (50 cm)	10 February 2021	CNES
12	SkySat-7 (50 cm)	26 February 2021	Planet Labs

evaluation, geomorphic indices such as Morphological Obstruction Index (MOI) and Hydro-morphological Dam Stability Index (HDSI) proposed by Stefanelli et al. (2016) were used.

$$\text{MOI} = \log (V_1/W_v) \quad (1)$$

$$\text{HDSI} = \log (V_1/A_b.S) \quad (2)$$

Where, V_1 is landslide dam volume (m^3), W_v is width of dammed valley (m), A_b is upstream catchment area (km^2) and S is local slope gradient of river channel (m/m). We have taken three scenarios of A_b : total upstream catchment area, 50% and 30% of upstream catchment area, to get information about the possible range of dam stability indices. According to Stefanelli et al. (2016), $\text{MOI} < 3.00$ is non-formation domain, $3.00 < \text{MOI} < 4.60$ is uncertain evolution domain and $\text{MOI} > 4.60$ is formation domain. Whereas $\text{HDSI} < 5.74$ is instability domain, $5.74 < \text{HDSI} < 7.44$ is uncertain determination domain and $\text{HDSI} > 7.44$ is stability domain.

Results

Rock avalanche

The main source of slope failure that triggered cascading effects in downstream areas is a rock avalanche which is clearly seen in the post-disaster image (Fig. 3). The crown of the rock avalanche is located at ~5474-m height and longitude $79^\circ 43' 52.03''$ E and latitude $30^\circ 22' 27.38''$ N. The rock avalanche has exposed three planar structural discontinuities. Comparison of the orientation of these discontinuities with the regional trend of the discontinuities revealed that two sets of joint planes and one foliation plane controlled the rock failure near the crown. These planes are well exposed in the Pleiades data. Traces of snow/ice melt water flow on these planar surfaces, which marks the direction of steepest

descent, were assumed as the dip directions of joint and foliation. Dip angle along the dip direction was measured by 3D interpretation of the satellite data. The dip direction/dip angles of Joint1, Joint2 and foliation are $350^\circ/79^\circ$, $295^\circ/62^\circ$ and $105^\circ/49^\circ$, respectively (Fig. 3). Photographs taken during the helicopter survey also show two sets of joints and a foliation plane (Fig. 4). The rock type at crown is migmatite gneiss and marble bands (Fig. 2). To understand the kinematics of the slope failure, the planar discontinuities were plotted on a stereonet (Fig. 5). The stereonet shows a typical wedge type failure controlled by Joint2 and Foliation (Goodman and Bray 1976; Hoek and Bray 1981). The average height and length of the head scarp are ~197 m and ~580 m, respectively. Head scarp and side scarps are clearly visible in the Pleiades image (Fig. 3). Fresh rocks and boulders are also clearly seen in the post event Pleiades image. All joints along the avalanche travel path were mapped (Fig. 1).

The release area (0.3 km^2), i.e. the rock and ice mass detached from the crown, was mapped from Pleiades images. Cut and fill analysis within the release area carried out using pre- and post-disaster DEMs estimated the volume of the landslide as ~29.3 million m^3 . Height of the release area was estimated by DEM differencing, and the maximum height (~197 m) of the release area was found near the head scarp (Fig. 6). WorldView-2 and Kompsat-3A images acquired in the same season, but with a gap of 5 years, clearly show the exposure of the joint plane (Fig. 5). The Resourcesat-2 image, which has minimal snow and ice cover, shows rock exposure within the release area (Fig. 5). The multi-temporal analysis of the rock avalanche zone shows gradual emergence of the joint that controlled the head scarp since the last 5 years. Freezing and thawing along the jointed rocks, which is prevalent in high altitude glaciated areas, has weakened the rock mass over a period of time. On 07 February 2021, maximum surface temperature reached ~278 °K from average maximum temperature of ~273 °K (ISRO 2021). Heavy snow fall during 02–06 February 2021 and increase in ambient temperature on 7 February 2021 possibly allowed percolation melt water in jointed rock

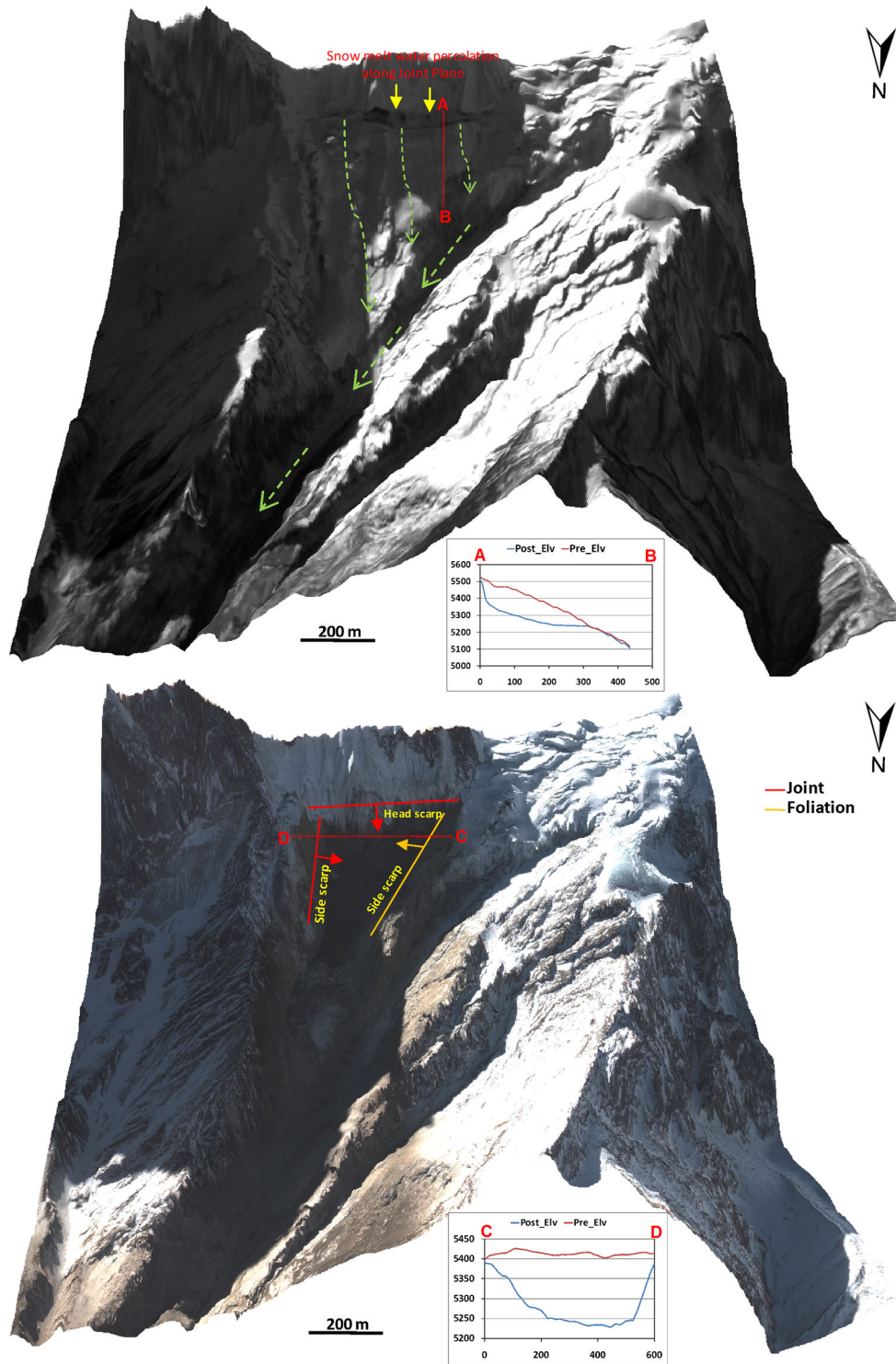


Fig. 3 3D perspective view of the rock avalanche. Insets show elevation profiles before (red) and after (blue) along A-B and C-D. Top — Cartosat-1 image showing the pre-failure surface. Dashed green arrows indicate the rock avalanche direction. Bottom — Pleiades image showing the post-failure surface. Scarps exposed due to wedge type failure along joint and foliation planes are clearly seen. Arrows (red and orange) indicate the dip directions of joint and foliation planes

mass which might have increased the pore water pressure and also enabled reduction of angle of internal friction for wedge type failure as seen in the stereonet (Fig. 5).

Air blast

Air blast is an extreme rush of air loaded with projectiles capable of causing severe destruction (Penna et al. 2020). Air blast is one of

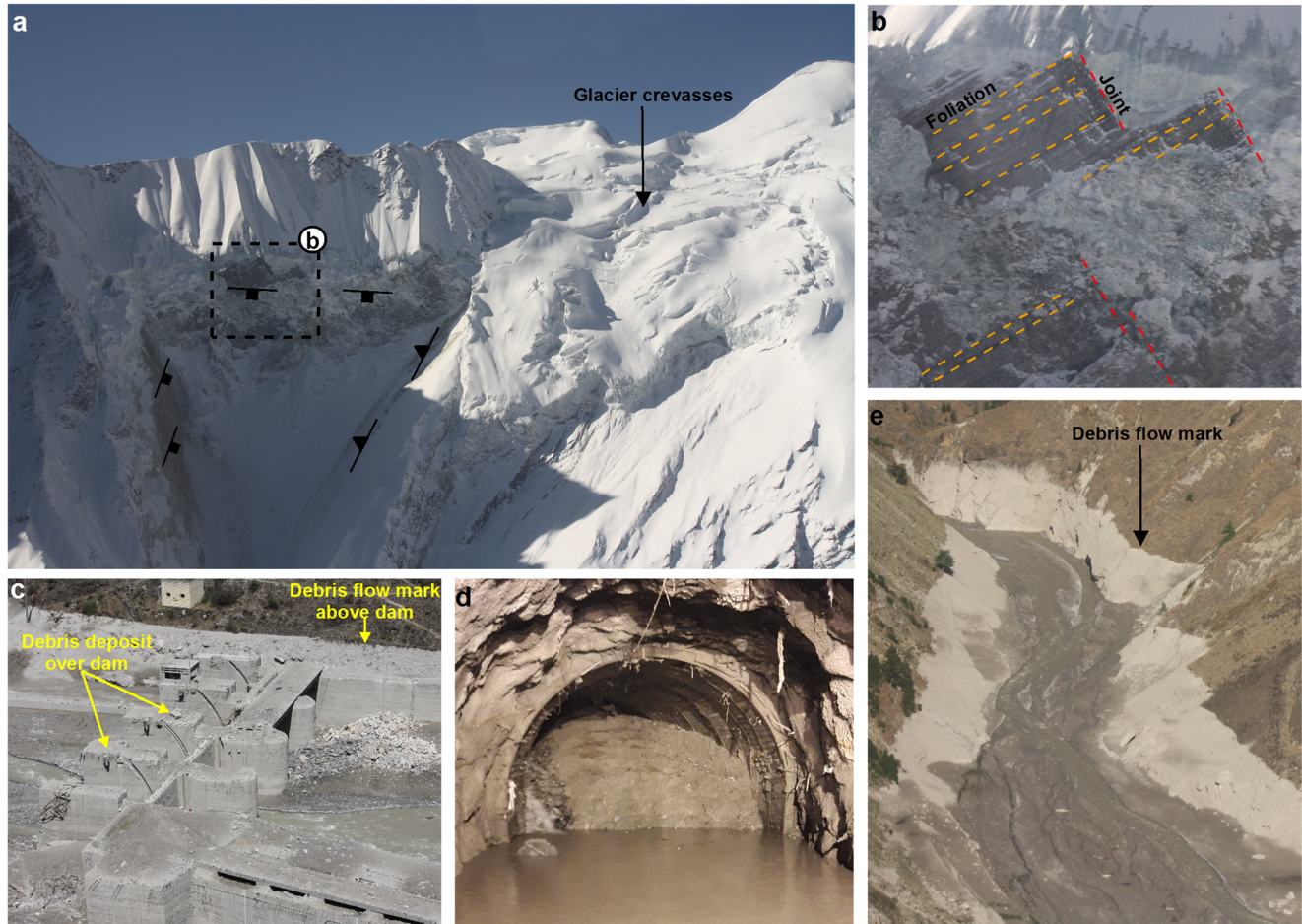


Fig. 4. a Photograph taken from the helicopter showing the triangle-shaped release area of the rock avalanche and a highly crevassed glacier on its right. Symbols show attitude of joint and foliation, b foliation and joint-1 exposed on the joint-2 section, c ground photograph showing boulders of various sizes over the dam and on the valley floor, d tunnel filled with debris and water wherein construction workers were trapped and e ground photograph showing debris flow mark above the valley floor

the prominent after effects of rock avalanche. The rock and ice mass that has descended from the crown region hit a mountain escarpment in the opposite side of the valley. The escarpment has approx. 900-m length and 500-m height, and it is oriented in the NNW-SSW direction. This vertical escarpment acted as a deflector and siphoned the displaced air mass towards the valley (Fig. 7). As a result of this air blast, trees were uprooted and snapped. The extent of damage to trees is seen up to 3.2 km from the zone of impact (Fig. 7). The path of air blast in the upslope region is shown in Fig. 8.

Debris bounce

The impact of rock and ice that crashed to the valley floor was such high that the pulverised rock mass and boulders jumped to the mountain opposite to the rock avalanche. Satellite data interpretation shows debris and boulders lying at an altitude of 4015 m which is ~285 m above the valley floor (Figs. 8 and 9).

Debris dam

The mass of rock and ice that fell on the Raunthi gad valley were pulverised due to high impact. The debris was strewn all over the crash zone and to the opposite valley wall. It is seen from the

satellite data interpretation that the debris deposited in the valley was removed partially on 07 February 2021, but still a large chunk of debris is lying in the valley (Fig. 10). This has blocked the valley completely by creating a debris dam. Minor accumulation of snowmelt water in the upstream of the debris dam is already visible in the image (Fig. 10). Since snowmelt is expected to increase in summer time, water will further accumulate here due to blockage of flow by the debris dam. The debris dam is unstable and cracks are visible on the top due to slumping. We have evaluated the stability of dam using two indices.

Landslide dam stability

The surface area of the landslide debris dam near the crash zone is ~29,630 m² with a length across and along the valley as ~185 m and ~155 m, respectively. The average height of the dam is ~20 m. The parameters used for the calculation of the MOI and HDSI indices are given in Table 2. Based on the MOI observation (MOI is 3.84), the area is observed to be in uncertain evolution domain. It indicates that the landslide dam is unstable. We have taken 3 scenarios of A_b , i.e. total upstream catchment area (65 km²), half upstream catchment area (32.2 km²) and one-third of upstream catchment area (21.6 km²) to derive the possible range of dam

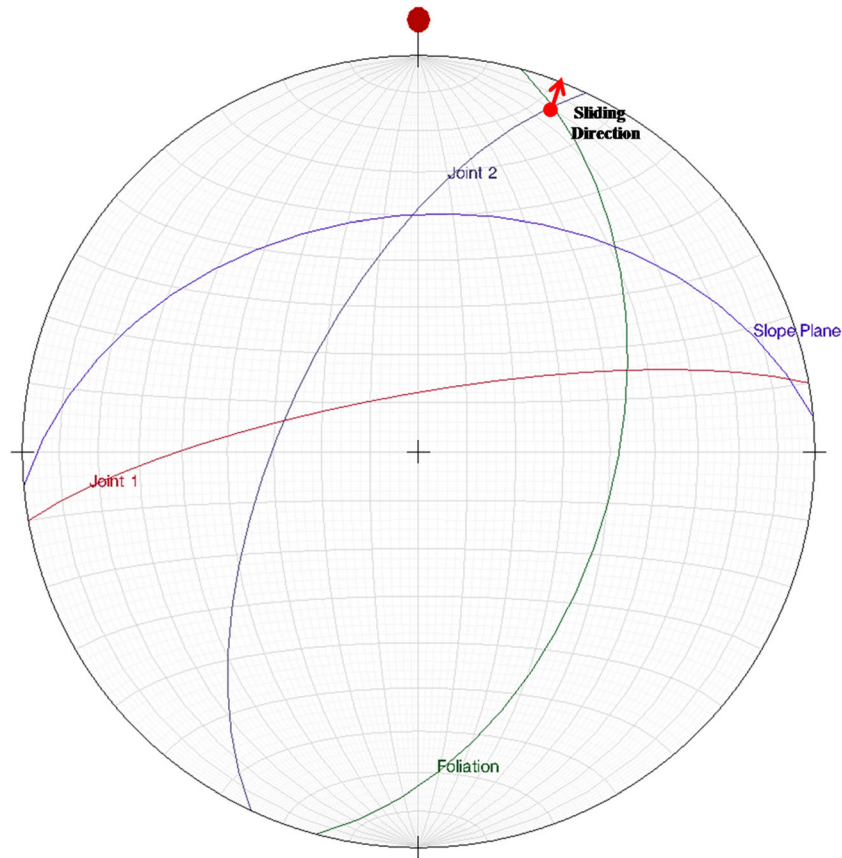


Fig. 5 Stereonet showing wedge type failure of the rock avalanche

stability index at three different scenarios. Based on the HDSI observation, for total upstream catchment area: HDSI is 5.42, for half upstream catchment area: HDSI is 5.72 and for one-third of the upstream catchment area: HDSI is 5.9. It is observed that the dam remains in the instability domain under total or 50% catchment contribution.

Discussion

The flash flood posed a unique challenge to scientists and researchers since the effect was observed for an unknown cause. The affected area is remote and not accessible on the ground; hence, satellite data were used to investigate the flash flood disaster. Pre and post change analysis coupled with photogeological study done using stereoscopic satellite imagery has shown that a rock avalanche has occurred along the western slope of Raunthi gad valley near the Raunthi peak. Analysis of pre-event imagery from Sentinel-2 satellite (05 February 2021) and Kompsat-3A (20 September 2020) shows an overhanging rock formation with joints near the crown. The geometry and orientation of the foliation plane and joints significantly control the consequent wedge type failure of the slope material (Fig. 5). The estimated volume of the landslide is ~ 29.3 million m^3 . This enormous volume of material impacting the valley floor has resulted in the massive air blast and debris bounce which is clearly illustrated from the satellite imagery. The accumulated debris has created an unstable dam as indicated by our estimation of MOI and HDSI values.

Debris mobilisation

The event witnessed a large amount of debris flowing in the Rishiganga-Dhauliganga valleys and subsequently in the Alaknanda river valley with a visible impact up to a distance of ~ 55 km from the crash zone. The debris mainly consists of ash grey colour clay with big to small size angular boulders (Fig. 4). The flow marks are clearly visible on the valley slope (Fig. 4). Satellite data analysis of the event near the crash zone did not show any geomorphic evidence of water impoundment. The large volume of failed rock and ice mass (~ 29.3 million m^3) were pulverised during the descent from ~ 5474 to ~ 3732 m and also by the crashing impact. The pulverised ice due to an increase in the surface area of small ice crystal had a greater chance of instantaneous melting because of frictional and impact heat. The ice melt water quickly got intermixed with the rock debris resulting in creation of slush at the crash zone, and since the shear strength of the slush is expected to be low, it could not withstand on a steep valley floor and thus started flowing downslope. The saturation further enhanced as the momentum of the flow increased.

Photogeological reconstruction of chain of events

The movement of debris flow with the frontal lobe was captured by the Planet-1 satellite at 10:31:51 h (IST) on 07 February 2017. The flow front has crossed the Raini village and started flowing in the Dhauliganga river (Fig. 11). A second image was captured by the satellite on the same day at 10:58:36 h (IST), and it is clearly seen that debris flow frontal lobe has

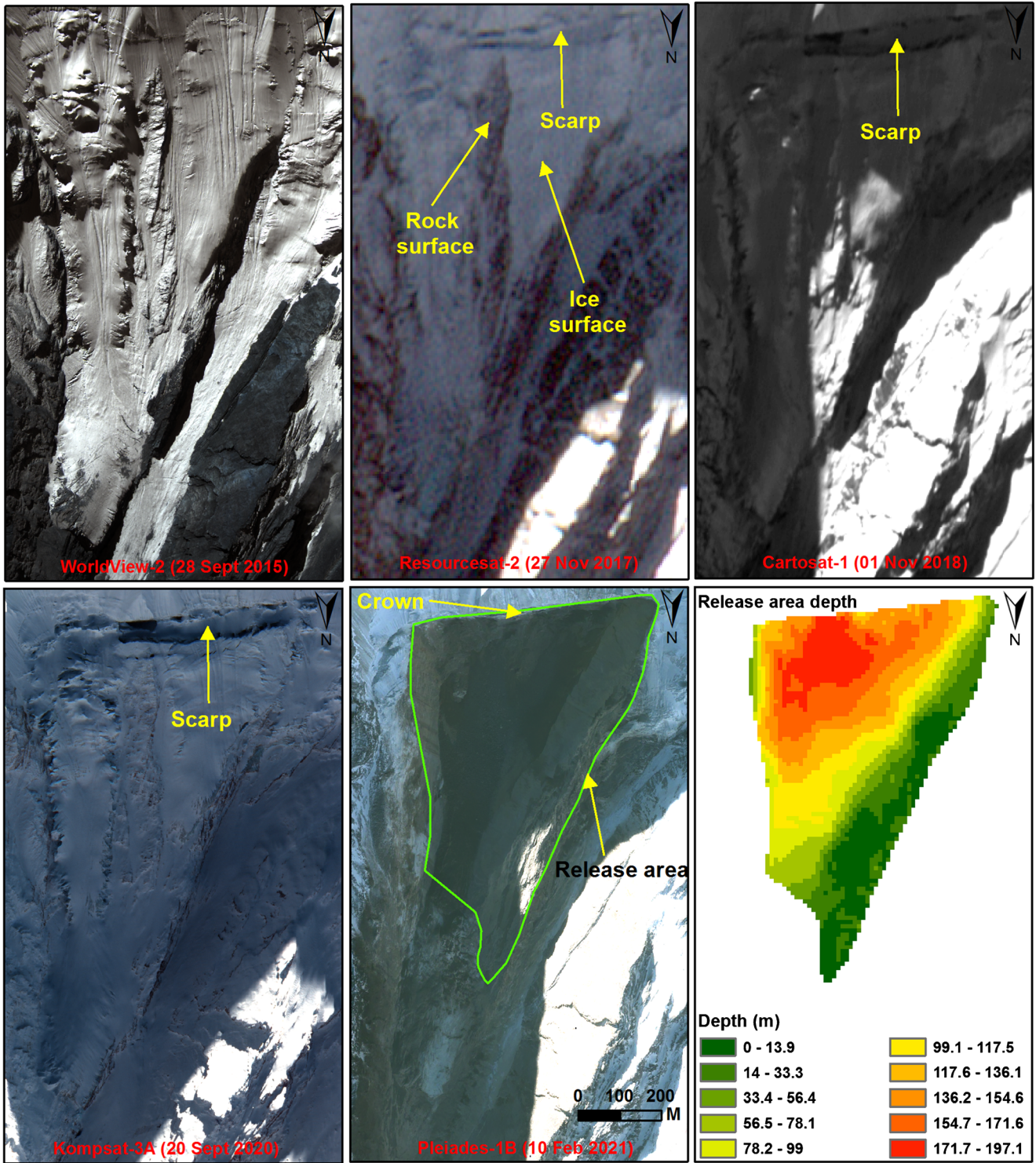


Fig. 6 Multi-temporal high-resolution image showing gradual emergence of the joint plane in the crown area. Landslide release area depth estimated from DEM differencing analysis is shown in a colour scale

crossed the Tapovan-Vishnugad hydel project located in the Dhauliganga river and reached Alaknanda river in the downstream. During this 00:27:15 h (T₁-T₂) period, the flow has travelled ~16,962 m. The average velocity thus estimated is 10.6 m/s. The velocity was assumed to be uniform and was used to estimate the origin time of the

debris flow at an upstream distance of ~14,688 m, i.e. crash zone from the first observed position (T₁) of the debris lobe. The time of flow initiation was estimated at 10:08:18 h (IST). The distance from the crash zone to the landslide lake that was formed at the confluence of Raunthigad and Rishiganga river is ~5183 m. Assuming the same uniform

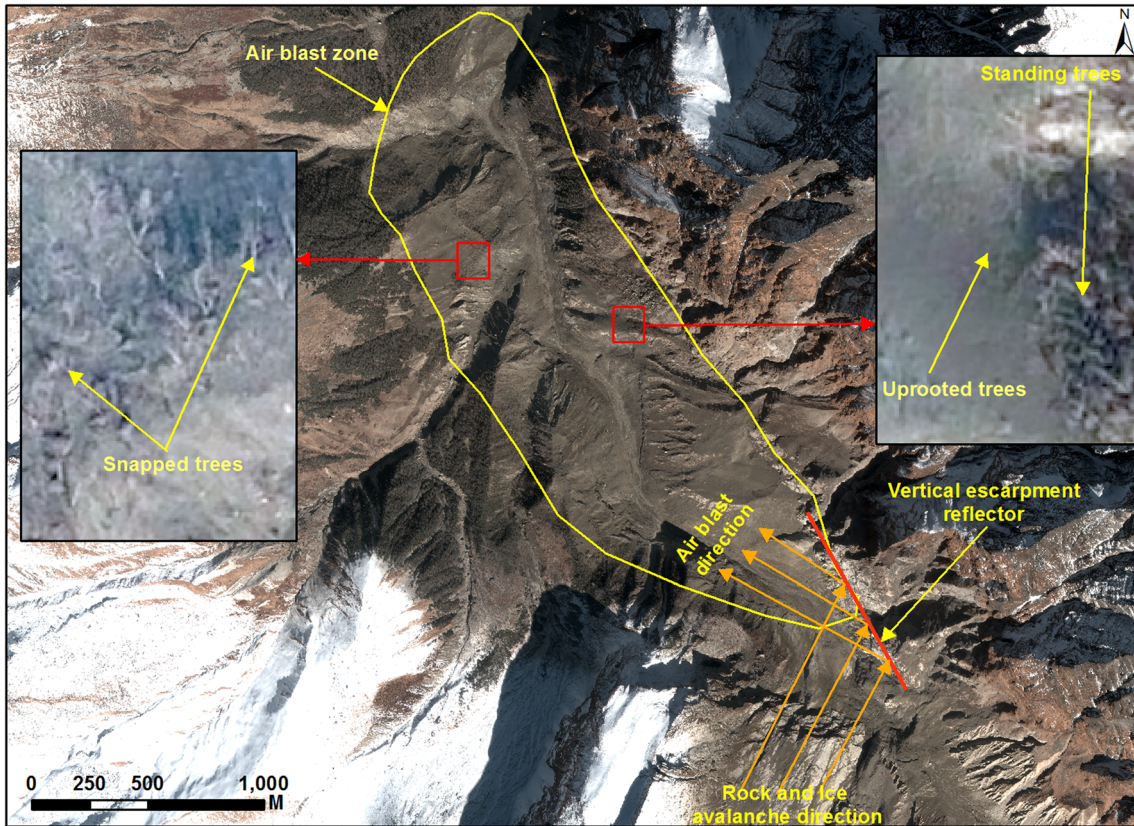


Fig. 7 Air blast due to rock and ice avalanche. Air blast zone and direction are illustrated on post-event Pleiades image. Two insets show snapped and uprooted trees due to air blast

velocity, it was estimated that the landslide dam and lake might have formed at 10:18:43 h. Planet-1 images also show varying intensity of dust

cloud near the crash zone and crown indicating that the rock avalanche continued for some time (Fig. 11).

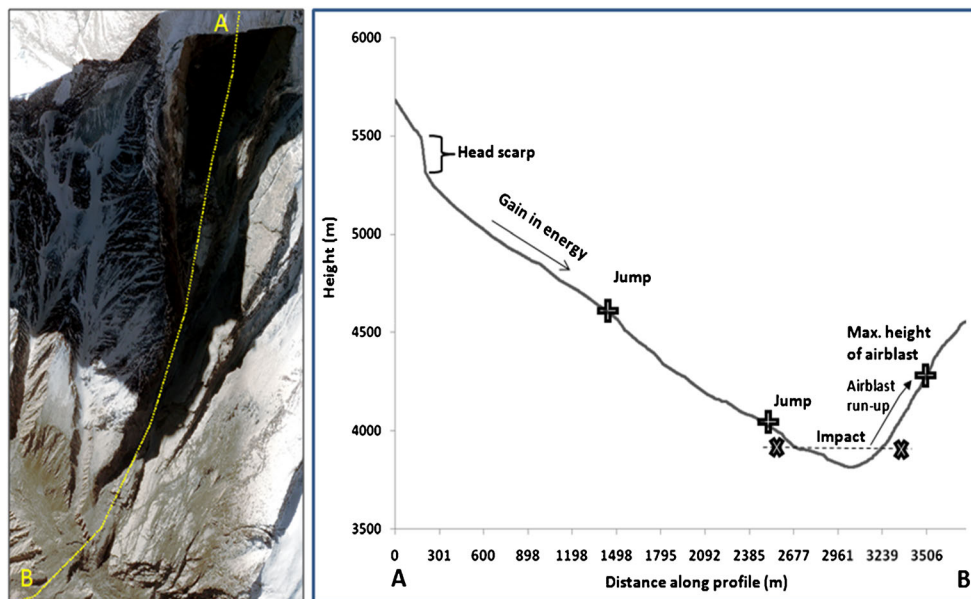


Fig. 8 Elevation profile along the travel path showing the behaviour of the rock avalanche. The profile line A-B is shown over the Resourcecesat-2 LISS IV image acquired on 08 February 2021

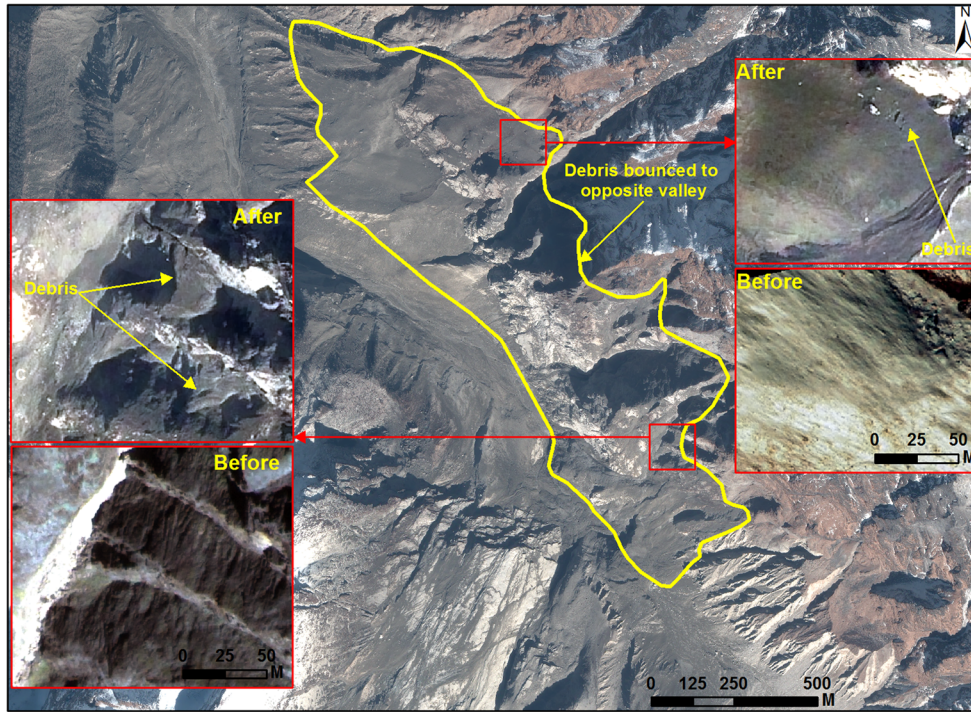


Fig. 9 Zone of debris deposition on the opposite valley wall is shown over the Pleiades image acquired after the disaster. The image before the disaster was acquired by Komsat-3A satellite

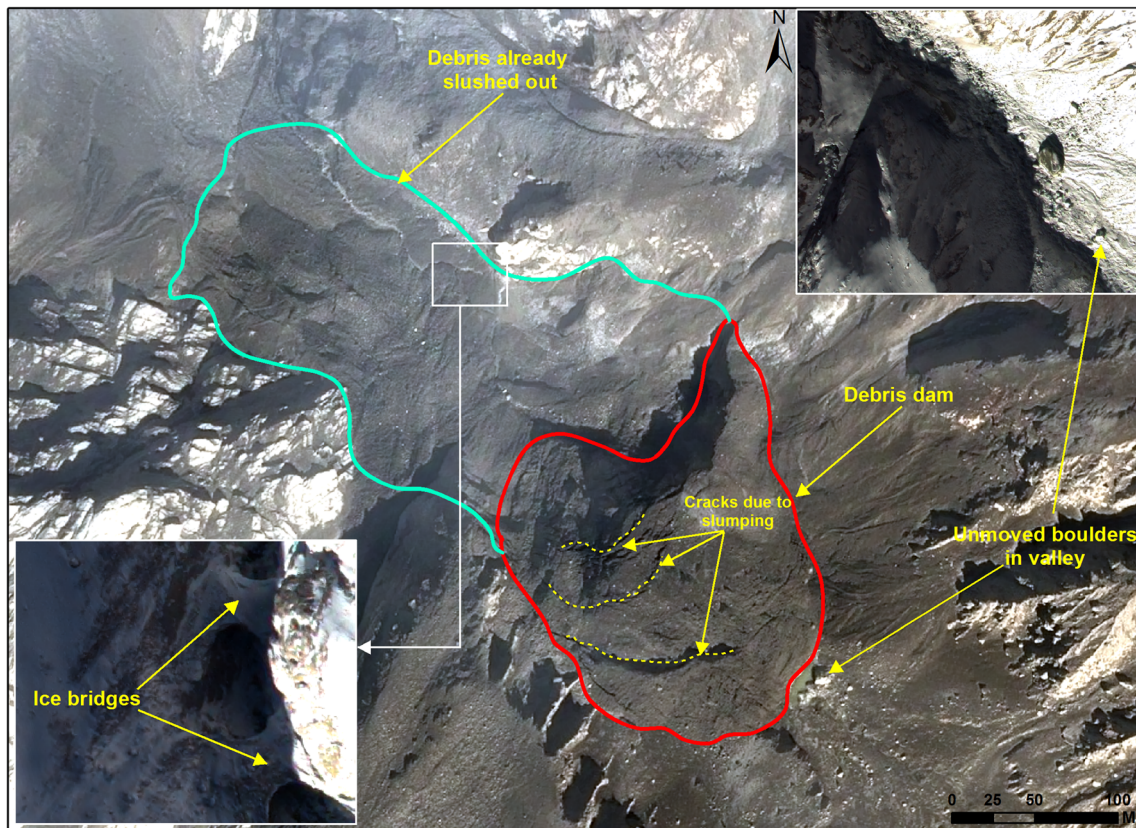


Fig. 10 Two potential hazard zones in the Raunthi gad valley mapped using Pleiades image. Pulverised chunk of debris blocking the valley. The red polygon shows the extent of the landslide debris that has blocked the Raunthi gad valley. Insets show pre-event high-resolution image of Komsat-3A

Table 2 Input parameter for Morphological Obstruction Index (MOI) and Hydro-morphological Dam Stability Index (HDSI)

Sl. no.	Parameter	Value	Index
1	V_l	592,600 m ²	MOI = 3.84
2	W_v	85 m	
3	A_b	Scenario 1: Total upstream catchment area: 65 km ²	HDSI = 5.42
4	A_b	Scenario 2: Half of upstream catchment area: 32.2 km ²	HDSI = 5.72
5	A_b	Scenario 3: A third of upstream catchment area: 21.6 km ²	HDSI = 5.90
6	S	29	

The above estimates of time along with geomorphic signatures and video footages of debris flow in downstream areas available in social media were used to derive the following sequence of events (time shown in IST) for the flash flood on 07 February 2021.

- i. *Few minutes before 10:08:45 h*—Rock avalanche occurred resulting in ice melting, air blast and dust cloud formation

near the crash zone. The rock avalanche dislodged more rocks along the travel path and then crashed to the Raunthi gad valley floor after travelling 2.9 km from the crown with a fall of approx. 1740 m. The high energy impact pulverised the rock and ice and created an air blast which snapped and uprooted trees up to 3.2 km in the downstream direction. The air blast also created dusts which have settled on the snow cover in the

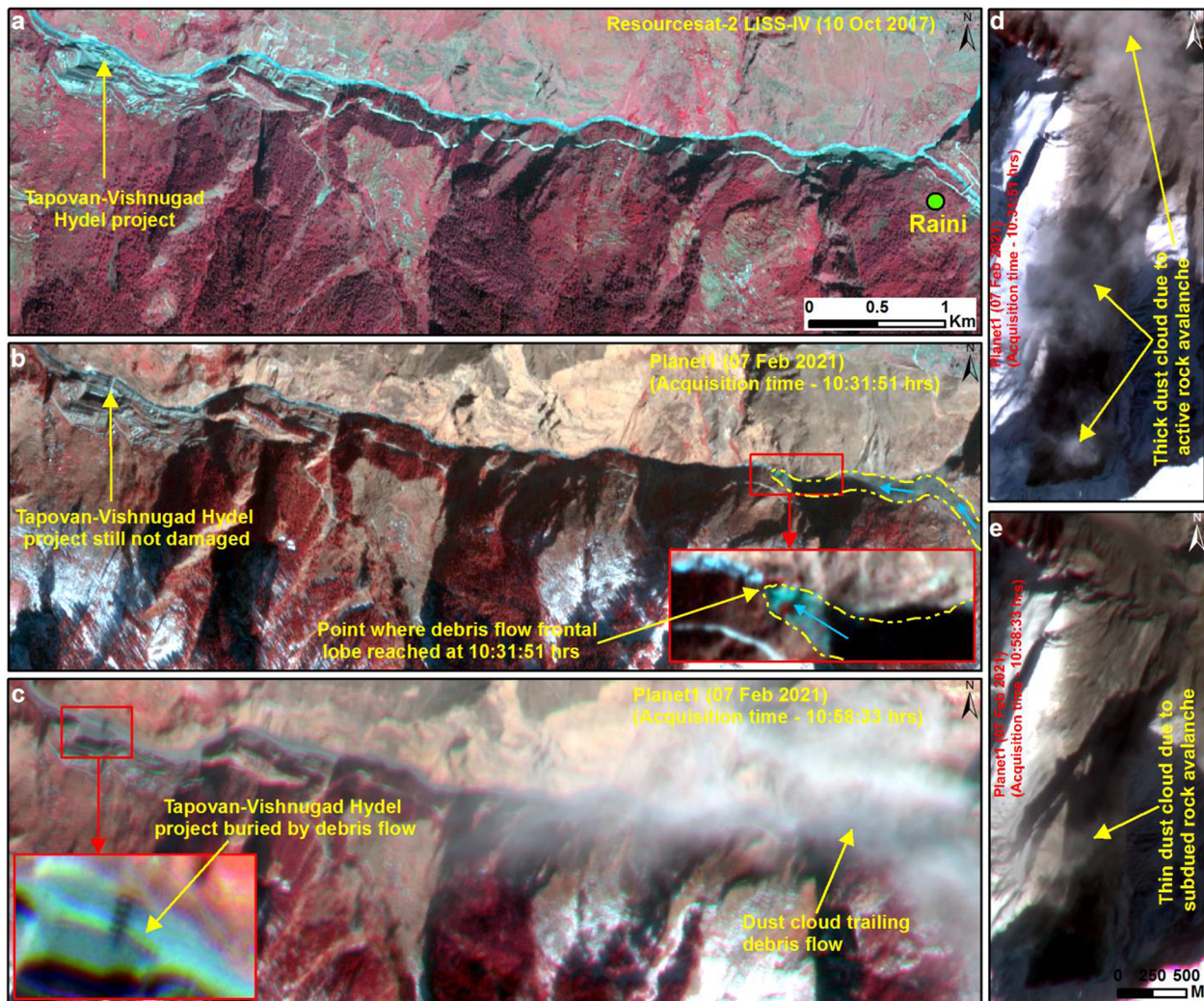


Fig. 11 Sequence of events derived using Planet-1 satellite data

- downstream side (Fig. 1). The debris also bounced to the top of the mountain in the opposite side of the valley up to a height ~ 285 m above the crash zone (Fig. 9).
- ii. 10:08:45 h—Debris flow started downstream from the crash zone, and the flow velocity is 10.6 m/s. As the slush moved down, it created more heat, and mobility of debris further increased due to entrainment. Majority of slush flowed downstream but left a chunk of debris in the valley resulting in formation of an unstable landslide debris dam near the crash zone in the Raunthi gad, which is vulnerable in the future. Currently minor impoundment is seen (Fig. 10) which may increase further in summer due to snow melt.
 - iii. 10:18:43 h—Debris blocked Rishiganga river at the confluence of Raunthi and Rishiganga and artificial lake formed thereafter. Currently, water is flowing over the landslide dam (Inset (b) in Fig. 1).
 - iv. 10:31:51 h—Active rock avalanche continued, and thick dust cloud is seen along the rock avalanche path and at the crash zone (Fig. 11). Debris flow reached the Dhauliganga river and subsequently buried the Tapovan-Vishnugad hydel project (Fig. 11).
 - v. 10:58:35 h—Thin dust cloud is seen near the crown, and no dust cloud is seen at the crash zone indicating that rock avalanche has subsided (Fig. 11). Duration of rock avalanching is ~50 min.>

Conclusion

We present a detailed geological assessment of the rock avalanche that triggered the flashflood in the Dhauliganga-Rishiganga valley. The stereo imagery from Pleiades satellite has provided an unprecedented synoptic view of the landslide area, affected valley floor and other regions in downstream areas. The wedge type failure of the rock mass was controlled by pre-existing set of joints along the rock face of the slope, which predominantly consists of fissile metamorphic rocks. The volume of the rock and ice mass is massive (~29.3 million m³) and thus is the high inherent potential energy at an altitude of ~5474 m. The rock avalanche released a huge amount of energy on impact, causing an air blast, pulverising material on the valley floor, melting large quantity of ice, resulting in debris flow which then inundated downstream dams and settlements. Such an event is hitherto less recorded in the Indian Himalayas and raises concerns over the stability of the glaciated high reaches of the Himalayan Mountains. The debris dam at the crash zone is analysed to be unstable which may be potentially hazardous in the forthcoming summer season. As a short-term measure, it is recommended that the debris dam near the crash zone needs to be monitored in forthcoming summer seasons since snow melt water can potentially create a lake which may breach the unstable landslide dam. In a recent study, Kumar et al. (2021b) found that the glaciated area in the Rishiganga catchment declined since 1980 as a result of deprived precipitation due to global warming. We have also found highly crevassed glaciers near the rock avalanche zone during the helicopter survey. Hence, as a long-term measure, in view of the global warming, monitoring large cracks and crevasses around the rock avalanche zone will help in assessing a similar type of failures in the future. The sequence of events, i.e. time stamping for the flash flood, was reconstructed based on the available satellite data till now and

may be further refined with availability of more ground and satellite data. The debris dam volume and rock avalanche volume presented in the report are estimated from satellite data using a photogrammetric technique in the best possible manner. The work presented in this paper has created baseline information for a disaster in a remote area and will help future work on flow simulation modelling. This study has also demonstrated the importance of multi-temporal high-resolution satellite data for assessment of disasters.

Acknowledgements

We thank Dr. Raj Kumar, Director, NRSC, for his support and guidance to this work. IRS satellite data were provided by NDC, and we thank them for their quick response. We thank GSI for sharing their preliminary report with NRSC. We would like to thank the International Charter for Space and Major Disasters for providing high-resolution satellite data acquired before and after the event that enabled us to carry out the work for the disaster that has occurred in an inaccessible and remote location in the Himalaya. We would also like to thank Dr. Shantanu Bhatawdekar, Director, EDPO and Dr. G Srinivasa Rao, Associate Director, EDPO for their active support to this study. We are extremely thankful to NDMA, SDRF, USDMA, NTPC and IAF for their support during the fieldwork. We are thankful to the suggestions of anonymous reviewers which has improved the research paper.

References

- Bhukosh 2021 www.bhukosh.gsi.gov.in
- Buss E, Heim A (1881) Der Bergsturz von Elm den 11. September 1881: Zurich, Wurster, 163 p
- Collins GS (2014) Rock avalanche. In: Encyclopedia of planetary landforms. Springer, New York. https://doi.org/10.1007/978-1-4614-9213-9_321-1
- Costa JE, Schuster RL (1988) The formation and failure of natural dams. *Geol Soc Am Bull* 100(7):1054–1068
- Dai FC, Lee CF, Deng JH, Tham LG (2005) The 1786 earthquake-triggered landslide dam and subsequent dam-break flood on the Dadu River, southwestern China. *Geomorphology* 65(3):205–221
- Delaney KB, Evans SG (2015) The 2000 Yigong landslide (Tibetan Plateau), rockslide-dammed lake and outburst flood: review, remote sensing analysis, and process modelling. *Geomorphology* 246:377–393
- Dong J-J, Li Y-S, Kuo C-Y, Sung R-T, Li M-H, Lee C-T, Chen C-C, Lee W-R (2011) The formation and breach of a short-lived landslide dam at Hsiaolin village, Taiwan—part I: Post-event reconstruction of dam geometry. *Eng Geol* 123:40–59
- Dunning SA, Mitchell WA, Rosser NJ, Petley DN (2007) The Hattian Bala rock avalanche and associated landslides triggered by the Kashmir Earthquake of 8 October 2005. *Eng Geol* 93(3-4):130–144
- Goodman RE, Bray JW (1976) Toppling of rock slopes. Proceedings, Speciality Conference on Rock Engineering for Foundations and Slopes. American Society of Civil Engineers (ASCE), Boulder
- Grodecki J, Dial G (2003) Block adjustment of high-resolution satellite images described by rational polynomials. *Photogramm Eng Remote Sens* 69:59–68
- GSI (2021) A Preliminary report on recent flash flood disaster in Rishiganga-Dhauliganga valley, Chamoli district, Uttarakhand, pp 21
- Gupta V, Sah MP (2008) Impact of the trans-Himalayan landslide lake outburst flood (LLOF) in the Satluj catchment, Himachal Pradesh, India. *Nat Hazards* 45(3):379–390
- Hoek E, Bray JW (1981) Rock slope engineering. The Institution of Mining and Metallurgy, London, p 358
- Huang D, Li YQ, Song YX, Xu Q, Pei XJ (2019) Insights into the catastrophic Xinmo rock avalanche in Maoxian county, China: combined effects of historical earthquakes and landslide amplification. *Eng Geol* 258:105158

- Hungro O, Evans SG (2004) Entrainment of debris in rock avalanches: an analysis of a long run-out mechanism. *Geol Soc Am Bull* 116(9-10):1240–1252
- ISRO (2021) Brief note on Uttarakhand flash floods—efforts of ISRO. pp 07
- Kargel JS, Leonard GJ, Shugar DH, Haritashya UK, Bevington A, Fielding EJ, Young N (2016) Geomorphic and geologic controls of geohazards induced by Nepal's 2015 Gorkha earthquake. *Science* 351(6269):aac8353
- Kumar V, Gupta V, Jamir I, Chatteraj SL (2019) Evaluation of potential landslide damming: case study of Urni landslide, Kinnaur, Satluj valley, India. *Geosci Front* 10(2):753–767
- Kumar V, Jamir I, Gupta V, Bhasin RK (2021a) Inferring potential landslide damming using slope stability, geomorphic constraints and run-out analysis; case study from the NW Himalaya. *Earth Surface Dynamics* 9:351–377. <https://doi.org/10.5194/esurf-9-351-2021>
- Kumar V, Shukla T, Mehta M, Dobhal DP, Bisht MPS, Nautiyal S (2021b) Glacier changes and associated climate drivers for the last three decades, Nanda Devi region, Central Himalaya, India. *Quat Int* 575–576:213–226
- Lagmay AMFA, Escape C, Ybañez AA, Suarez JK, Cuaresma G (2020) Anatomy of the Naga City landslide and comparison with historical debris avalanches and analog models. *Front Earth Sci* 8:312
- Li T, Schuster RL, Wu J (1986) Landslide dams in south-central China. In: *Proc. Landslide dams: processes, risk, and mitigation*. ASCE Convention, Washington, pp 146–162
- Martha TR, Vinod Kumar K (2013) September, 2012 landslide events in Okhimath, India—an assessment of landslide consequences using very high resolution satellite data. *Landslides* 10:469–479
- Martha TR, Kerle N, Jetten V, van Westen CJ, Vinod Kumar K (2010) Landslide volumetric analysis using Cartosat-1-derived DEMs. *IEEE Geosci Remote Sens Lett* 7:582–586
- Martha TR, Roy P, Babu Govindharaj K, Vinod Kumar K, Diwakar PG, Dadhwal VK (2015) Landslides triggered by the June 2013 extreme rainfall event in parts of Uttarakhand state, India. *Landslides* 12:135–146. <https://doi.org/10.1007/s10346-014-0540-7>
- Maskey S, Kayastha RB, Kayastha R (2020) Glacial lakes outburst floods (GLOFs) modelling of Thulagi and Lower Barun glacial lakes of Nepalese Himalaya. *Prog Disaster Sci* 7:100106. <https://doi.org/10.1016/j.pdisas.2020.100106>
- Penna IM, Hermanns RL, Nicolet P, Morken OA, Dehls J, Gupta V, Jaboyedoff M (2020) Air blasts caused by large slope collapses. *GSA Bulletin* 133(5-6):939–948. <https://doi.org/10.1130/B35531.1>
- Shrestha AB, Eriksson M, Mool P, Ghimire P, Mishra B, Khanal NR (2010) Glacial lake outburst flood risk assessment of Sun Koshi basin, Nepal. *Geomatics Nat Hazards Risk* 1(2):157–169. <https://doi.org/10.1080/19475701003668968>
- Stefanelli CT, Segoni S, Casagli N, Catani F (2016) Geomorphic indexing of landslide dams evolution. *Eng Geol* 208:1–10. <https://doi.org/10.1016/j.enggeo.2016.04.024>
- Takahashi T, Nakagawa H (1993) Flood and debris flow hydrograph due to collapse of a natural dam by overtopping. *Proc Hydraul Eng* 12(2):41–49. <https://doi.org/10.2208/prohe.37.699>
- Vinod Kumar K, Lakhera RC, Martha TR, Chatterjee RS, Bhattacharya A (2008) Analysis of the 2003 Varunawat landslide, Uttarkashi, India using earth observation data. *Environ Geol* 55:789–799
- www.ndtv.com. Accessed on 8th February 2021
- Žáček V, Bohdál P, Břízová E, Buriánek D, Čáp P, Enkhjargal M, Čopjaková R (2017) Mongol Altai 50—a development cooperation project of Czech Republic with Mongolia in geology (2013–2016). *Geosci Res Rep* 50:159–166

T. R. Martha (✉) · P. Roy · N. Jain · K. Vinod Kumar · P. S. Reddy · J. Nalini · S. V. S. P. Sharma · A. K. Shukla · K. H. V. Durga Rao · B. Narender · V. N. Rao · S. Muralikrishnan
 National Remote Sensing Centre (NRSC),
 Indian Space Research Organisation (ISRO),
 Hyderabad, 500 037, India
 Email: tapas_martha@nrsc.gov.in; trmartha@rediffmail.com